SPACE Conferences & Exposition
4-7 August 2014, San Diego, CA
AIAA/AAS Astrodynamics Specialist Conference

Trajectory Optimization for Adaptive Deployable Entry and Placement Technology (ADEPT)

Sarag J. Saikia[1], Harish Saranathan[2], Michael J. Grant[3], James M. Longuski[4]
School of Aeronautics and Astronautics, Purdue University, 701 W. Stadium Ave., West Lafayette, IN 47907-2045

Large-scale human exploration of Mars, and in situ exploration of Venus pose great challenges for entry, descent, and landing of spacecraft. The Adaptive Deployable Entry and Placement Technology (ADEPT), a mechanically deployable decelerator, presents an enabling alternative to the traditional rigid aeroshell technology. ADEPT helps in lowering the ballistic coefficient of an entry vehicle and also presents attractive options for lifting and guided entry. Optimal trajectory solutions which minimize peak deceleration and peak heat-flux are computed for four different control strategies. The deployable decelerator for human Mars missions (requiring a landed mass of 40 mt) presents an acceptable entry environment—peak heat-flux of < 80 W/cm^2, and peak deceleration of less than 4 *g* (compared to 200 W/cm^2 and 15 *g* for Mars Science Laboratory respectively). For lifting and guided entry for Venus in situ missions, ADEPT could lead to a two-order-of-magnitude decrease in peak deceleration and to a 50% decrease in peak heat-flux compared to conventional rigid aeroshell technology.

Nomenclature

β	=	ballistic coefficient of an entry vehicle, kg/m^2
C_D	=	drag coefficient
A	=	reference area of the entry vehicle, m^2
β	=	flight path angle, degrees
$\eta_{\max}$	=	peak deceleration in Earth *g*
$q_{\max}$	=	peak convective heat flux, W/cm^2
J	=	Objective function of the optimal control problem
t_f	=	final time, s
k	=	thermal conductivity, W/m-K
ρ	=	density of the atmosphere, kg/m^3
R_n	=	nose-radius of the spacecraft, m
V	=	velocity of the spacecraft, m/s
η_c	=	constraint on peak deceleration in Earth *g*
$u(t)$	=	control variable

[1] Ph.D. Candidate, School of Aeronautics and Astronautics, 701 W. Stadium Ave., West Lafayette, IN 47907, and AIAA Student Member.
[2] Graduate Student, School of Aeronautics and Astronautics, 701 W. Stadium Ave., West Lafayette, IN 47907, and AIAA Student Member.
[3] Assistant Professor, School of Aeronautics and Astronautics, 701 W. Stadium Ave., West Lafayette, IN 47907, and AIAA Member.
[4] Professor, School of Aeronautics and Astronautics, 701 W. Stadium Ave., West Lafayette, IN 47907, and AIAA Associate Fellow, AAS Member.

I. Introduction

HUMAN missions to Mars, and in situ missions to Venus pose great challenges for entry, descent, and landing (EDL) of spacecraft that can not be overcome by conventional rigid aeroshell technology. The challenges exist for entry on both Mars and Venus for unique reasons. For Mars challenges are due to an atmosphere—surface density of around 0.02 kg/m^3—thick enough to create substantial heating, but not sufficiently high enough deceleration. On the other hand, Venus has an extremely thick atmosphere atmosphere with a surface density of around 65 kg/m^3, which presents a high heat flux and high pressure entry environment. At the heart of the EDL problems on Mars and Venus, is the need to reduce the ballistic coefficient of the entry vehicle. The ballistic coefficient of an entry vehicle is defined by

$$\textit{Ballistic Coefficient } (\beta) = \frac{m}{AC_D} \ \frac{kg}{m^2} \tag{1}$$

where, m is the mass, C_D the drag coefficient, and A, the reference surface area of the entry system respectively. Thus, for a given mass, β is inversely proportional to the drag-area of the entry vehicle. from a dimensional analysis of Eq. (1), it is clear that Dim[β] = l^3/l^2 = l. Thus the ballistic coefficient increases with characterisitic length (size), which is the reason that heavy landers get less atmospheric assistance during landing. For low $-\beta$ vehicle, deceleration occurs at much higher altitudes, thereby lowering peak g-load, heat rate, aerodynamic pressure, and total heat load.

Large-scale scientific and human exploration of Mars will require an order of magnitude enhancement in landed-mass capability—40 mt to 80 mt at scientifically interesting sites[1]. The Entry, Descent and Landing (EDL) technology employed for all the missions to Mars till date is based on that developed for the Viking program in the 1970s. However, the limit of Viking era rigid aeroshell technology is around 1–2 mt on the surface of Mars. To fulfill such requirements of human exploration of Mars requires new EDL technologies and methods. Some of the challenges of precision landing of payloads as large as 40 mt on the surface of Mars have been studied by NASA[2]. In a follow-up study[3], larger payloads (about 80 mt) are considered that include an aerocapture followed by an EDL via a deployable aerodynamic decelerator. Dwyer-Cianciolo et al. conclude that deployment of a 23-m Hypersonic Inflatable Aerodynamic Decelerator (HIAD) for aerocapture, followed by a 44-m Supersonic Inflatable Aerodynamic Decelerator (SIAD) for the supersonic descent regime would be required to deliver 40 mt on the surface of Mars where the arrival mass is about 80 mt). On the other hand, a rigid aeroshell would require an arrival mass of about 114 mt (and a prohibitive rigid aeroshell size) to deliver the same payload mass[2, 3].

The Russian Venera and Vega; and America's Pioneer Venus (PV) are the only probe missions to survive the harsh entry environment on Venus. All the past missions to Venus have used rigid aeroshells (sphere, circumellipsoid, and sphere-cone designs) technology.[4] However, Venus' thick atmosphere subjects the entry vehicle to large peak-heat fluxes and high peak-deceleration loads. The heritage US entry vehicle for Venus is the $45°$ sphere-cone rigid aeroshell. The size of a rigid aeroshell technology is inhibited by the payload fairing diameter of the launch vehicle. Thus, payload fairing constraints the minimum achievable ballistic coefficient, β, to a value higher than 100 kg/m^2.

In the only US mission to Venus, Pioneer-Venus, the Thermal Protection System (TPS) consisted of fully dense Carbon Phenolic (CP)[4]. Carbon Phenolic was originally developed as a rocket nozzle throat material, and is the only material with flight heritage for the high heat-flux and high pressure that Venus presents. Carbon Phenolic is a high density material and characterized by high thermal conductivity. Given these characteristics, the vehicle (with β =190 kg/m^2) enters at steep entry flight path angles, γ, to shorten the peak heat-flux which leads to the increase in the total heat load. For PV, entry flight angles fall in the range $-25.4° \le \gamma \le -68.7°$ with an entry velocity of 11.5 km/s. These entry conditions lead to very high peak heat fluxes in the range $5.2\ kW \le q_{\max} \le 10.6\ kW$; and very high peak deceleration in the range, $219\,g \le \eta_{\max} \le 487\,g$! Dutta et al. show that when the ballistic coefficient is lower (~30 kg/m^2), much shallower entry flight angles becomes practicable that leads to order of magnitude reduction in peak heat flux and peak deceleration load.[4]

A mechanically-deployed aerodynamic decelerator, known as the Adaptive Deployable Entry, and Placement Technology (ADEPT), is considered as a viable alternative entry system technology that can provide great benefits as opposed the conventional rigid aeroshell technology. Using ADEPT, the ballistic coefficient can be reduced via the in-space deployment of a high-temperature capable decelerator, which increases the reference surface area of the entry vehicle. NASA's Office of the Chief Technologist has funded a study of the rigid deployed hypersonic

decelerator system. The ADEPT architecture provides a breakthrough for future human missions to Mars, and robotic missions to Venus. The viability of ADEPT for heavy-mass Mars entry problem, as well as low-β, shallow-γ, entries on Venus has been studied.[5-6]

II. Motivation

Past probe entry missions incorporated bank angle modulation alone (e.g. Apollo and THE Mars Science Laboratory), a combination of bank angle and angle of attack (e.g the Space Shuttle), or no control at all (e.g. Mars Exploration Missions, Mars Phoenix Mission, and the Stardust). Until now, only ballistic entries have been considered for ADEPT architecture.[5,6] However, ADEPT has the capability to simultaneously incorporate bank angle, angle of attack, and drag modulation for lifting and guided entry, which will further help to present a benign entry environment. Therefore, it is essential that the control strategies are studied and compared to get the best choice for a given mission objective. From a guidance standpoint, the capability to control angle of attack, bank angle, and drag has the advantage of precision landing in the presence of navigation errors and atmospheric perturbations. The goal of this work is to assess various control strategies for the computation of optimal trajectories of ADEPT for entry on Mars and Venus.

III. Baseline Mission Concepts

A. Human Missions to Mars

The viability of ADEPT concept for heavy-mass Mars missions has been analyzed in the Entry, Descent, and Landing—Systems Analysis (EDL-SA) architecture studies.[2,3] The proposed mission architecture constitutes a multitude of Earth launches providing necessary cargo followed by human on Mars surface. Based on the EDL-SA study, four EDL architectures were developed and analyzed for ADEPT.[5] The different phases of the architectures are: launch, deploy hypersonic decelerator, cruise, aerocapture, secondary deployment, entry, attitude control, supersonic flight, supersonic retro-propulsion, ejection of decelerator, subsonic retro-propulsion, and terminal landing. Depending on the architecture, certain phases are not relevant. The phases are described in detail by Venkatapathy et al. in Ref. 5.The four ADEPT architectures are shown in Fig. 1.

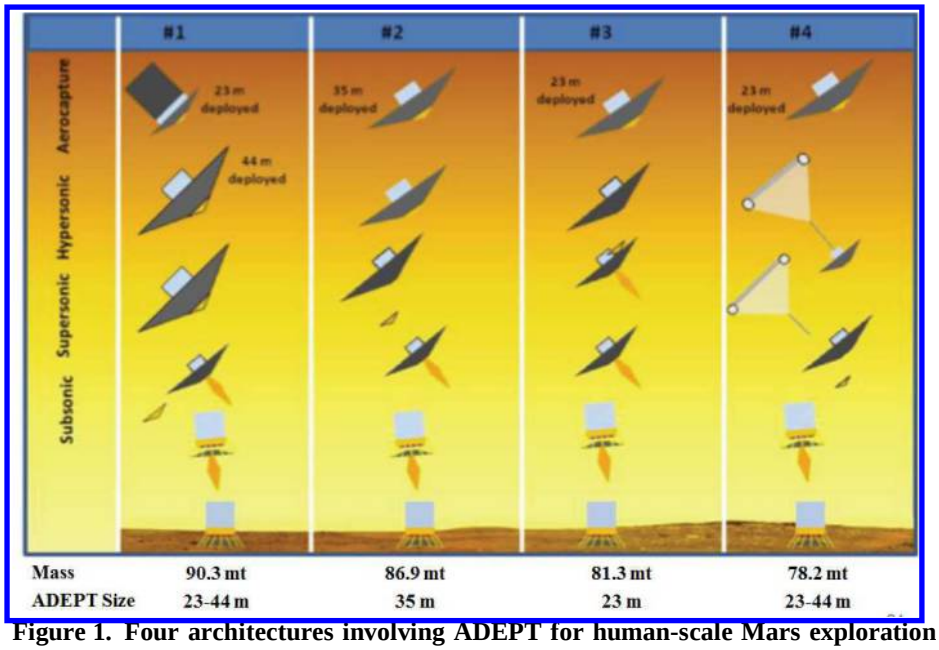

Figure 1. Four architectures involving ADEPT for human-scale Mars exploration with a payload mass of 40 mt. The four architectures are derived from NASA EDL-SA study led by Dwyer-Cianciolo,[2,3] but differ primarily in the size of the decelerator and in the method used for deceleration during supersonic phase.

Two discrete deceleration maneuvers are included in the nominal mission architecture (1) aerocapture to orbit (2) entry from orbit.[5] Supersonic retro-propulsion is used for terminal descent as well as for precision landing. Therefore, the ADEPT is used for deceleration only in the hypersonic and supersonic regimes, as shown in Fig. 1. The key difference between the four architectures is how each of them manages the supersonic phase. Except #2, all the other architectures use 23 m ADEPT for aerocapture; and all the architectures use subsonic retropropulsion for terminal descent. Supersonic retropropulsion is common to architectures #1, #2, and #3. For this paper, optimal lifting and guided trajectories of ADEPT are computed for direct entry from orbit for the architectures #1 and #3.

B. Venus In Situ Missions

The priority science questions for Venus have been identified in the 2013 National Research Council's (NRC) Planetary Decadal Survey.[7] European Space Agency's (ESA's) Venus Express is currently in orbit observing polar cloud dynamics and composition and is helping in the understanding of the structure, chemistry, and dynamics of the atmosphere. The gaps in the knowledge of the atmosphere to understanding climate evolution of Venus will require in situ measurements of deep atmospheric gas compositions and surface mineralogy that can be obtained using landers that can survive entry in to the dense Venusian atmosphere. As a part of the NRC's Decadal Survey, Venus Intrepid Tessera Lander (VITaL) mission concept is designed to land on the tesserae terrain and achieves the New Frontiers science objectives.[7]

Figure 2 shows the VITaL lander repackaged in to the ADEPT structure of a 6 m / 70º diameter ADEPT-VITaL configuration. The feasibility, risks, benefits, and limitations of the ADEPT mission (with the VITaL lander repackaged into ADEPT) are outlined in Ref. 8, where a mass saving of 248 kg is achievable compared to the baseline VITaL Current Best Estimate of 1061 kg.[8] In the baseline mission concept, the lander lands on a tessera region (study baseline is Ovda Regio, 3.7º E longitude, and, 25.4º S latitude) and carries the same instruments as VITaL lander and fulfil the same scientific objectives. The mission concept provides measurements of: (a) surface chemistry and mineralogy (b) important atmospheric species that can answer fundamental questions about the evolution of Venus. (c) noble and trace gases (d) potential crustal dipole magnetic field.[7] The entry mass of ADEPT-VITaL is 1602 kg and it carries the payload from entry interface to subsonic (Mach 0.8) parachute deployment at around 75 km. The parachute extracts the lander from ADEPT Decelerator for terminal descent and landing.

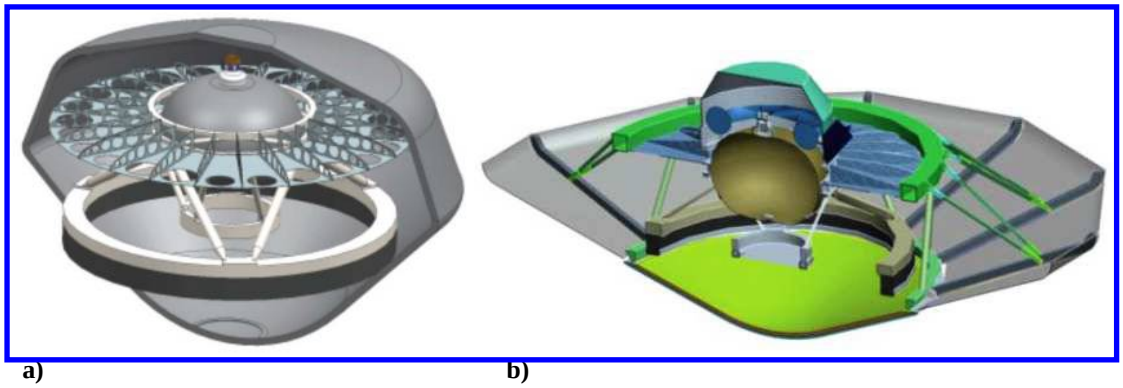

a) **b)**

Figure 2. a) Cross sectional view of baseline VITaL, b) ADEPT-VITaL configurations. VITaL is a 3.5 m / 45º sphere-cone, and ADEPT-VITaL is a 6 m / 70º diameter decelerator[6]. ADEPT for heavy-mass Mars missions has very similar features.[6]

Ballistic entry for ADEPT showed that the peak deceleration could be reduced by an order of magnitude to 30 *g* (compared to >220 *g* for Pioneer-Venus) and peak heat flux to 300 W/m^2 (compared to > 5.2 kW/cm^2 for Pionner-Venus). The peak deceleration of 30 *g*, is still higher compared to other probe entries on Mars and Titan. Higher g's requires more mass for structure and instruments. However, with lifting and guided entry could further reduce the deceleration and heat-flux loads, thus mass.

IV. ADEPT Concept Description

The low ballistic coefficient of ADEPT is achieved by mechanically-deployable semi-rigid aeroshell. At the heart of this architecture is a mechanically deployable aerodynamic surface (aeroshell), analogous to an umbrella. During launch, the aero surface is stowed to fit into the payload fairing of the launch vehicle. It is then deployed in Earth orbit to provide a large aerodynamic surface during EDL on the target planet. The structural skeleton of ADEPT is comprised of four principal subsystems: main body, nose cap, ribs, and struts, as shown in Fig. 3a. The nose cap is a traditional 70° sphere-cone aeroshell with a base diameter of required diameter for a mission type. For ADEPT-VITaL[6] the base diameter is 3 m, and for human Mars mission, the base diameter varies from 23 m to 44 m with 40 mt payload[5]. The ribs provide support to the tensioned 3D-woven carbon cloth as the thermal protection system, and a pair of struts in turn supports each rib against aerodynamic loads. The nose cone shape provides the switch to the faceted pyramid shape of the rib and carbon cloth portion of the aeroshell. The nose cone uses Phenolic Impregnated Carbon Ablator (PICA) as the TPS material.[6] For Mars missions, as shown in Fig. 3a the nose cone

jettisons to expose the supersonic retropropulsion elements for terminal descent, accommodated entirely within the structure. More detailed descriptions of ADEPT concept for Mars and Venus can be found in Refs. 5 and 6.

The main body, shown in Figs. 3b and 4a, consists of an upper and a lower rings: the upper ring supports the

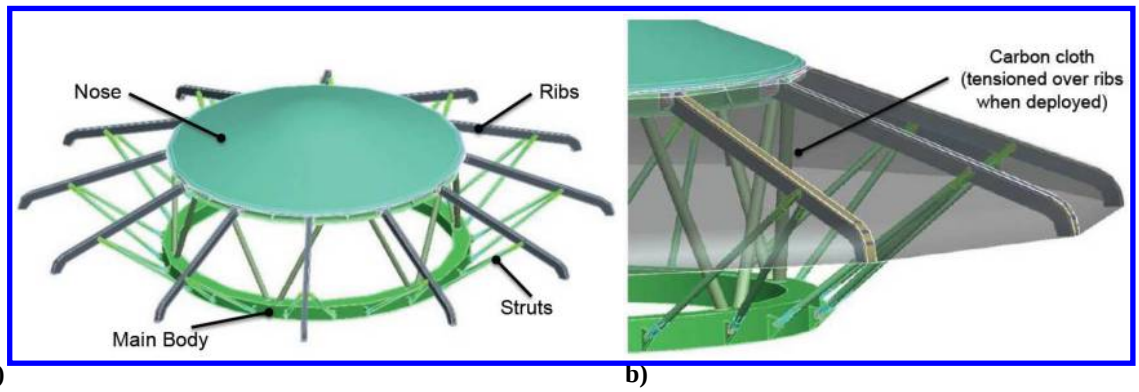

a) **b)**

Figure 3. a) ADEPT skeleton showing the four primary subsystems: main body, nose cap, ribs, and struts. b) tensioned 3D woven carbon cloth over ribs of ADEPT when fully deployed.[6]

landing ring (for VITaL), serves as a structure to attach the nose cap, or as a structure for the supersonic retropropulsion elements for Mars missions as shown in Figure 3 and 4. The lower ring serves as the adapter for payload and cruise stage interface.

Figure 4 also shows the three primary configurations of ADEPT: stowed, deployed, and landing. After the function of decelerator is complete, the decelerator is inverted to function both as a landing attenuation system and as a debris shield.[5] Among the mechanisms, the primary one is a motor-driven winch and cable system for the

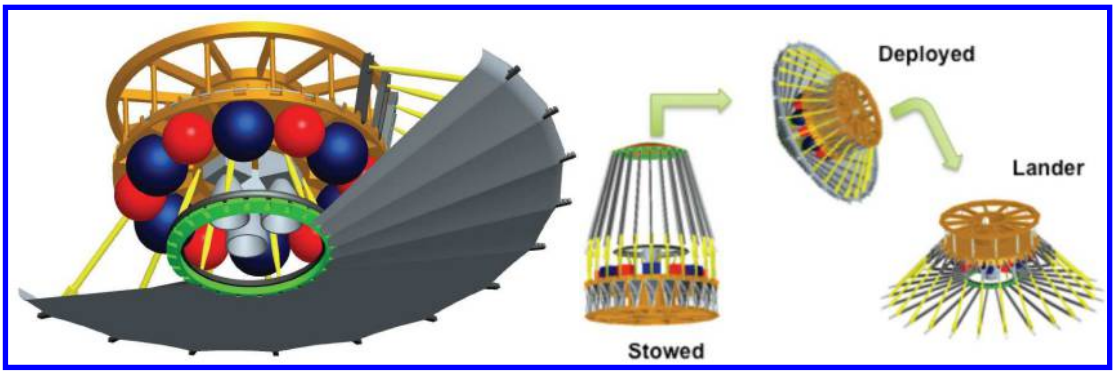

a) **b)**

Figure 4. a) ADEPT for Mars mission with a view of supersonic retropropulsion system b) three ADEPT configurations when stowed, deployed, and for landing for Mars missions.[5]

deployment of the decelerator. A detailed description of the mechanism can be found in Ref. 6. Drag modulation by changing the decelerator deployment angle, is one of the additional control strategies considered (see Section V on Control Strategies). It is assumed that the same motor-driven winch and cable system mechanism can be used to for the control of the decelerator deployment angle actively during entry. However, no additional mass is considered in computing the ballistic coefficient. In reality, there will be a small mass penalty.

The aerodynamics surface—grey surface in Fig. 4a— is formed by the tensioned 3D-woven cloth over the ribs.The carbon cloth is capable of operating at temperatures in excess of 1600º C, thereby precluding the need of additional TPS materials.[6, 9] A detailed entry aerothermal analysis of ADEPT-VITaL can be found in Ref. 6 and that of ADEPT-Mars can be found in Ref. 5.

V. ADEPT Control Strategies

The primary control method conceived for ADEPT is the angle of attack and bank angle, which can be achieved via the gimballing of the aerodynamic surface.[5] Additional control methods are considered to understand their effectiveness for different entry problems. Four different control methods are summarized in this section for human Mars missions. For Venus in situ missions, the legacy bank angle control method is included instead of modified drag control.

A. Angle-of-Attack and Bank Angle

The originally designed control method for ADEPT is to gimbal the aerodynamic surface. Gimbaling of the aeroshell results in a shift in the center-of-mass relative to the aeroshell's axis of symmetry. The shit in center-of-mass results in a non-zero trim angle-of-attack, which producesn aerodynamic lift. The lift vector can be pointed in the desired direction by suitably gimbaling the aeroshell. This can be deduced into a unique combination of angle-of-attack and bank angle. The maximum excursion angle is 12.5 degrees, with a corresponding trim angle-of-attack of 27 degrees. Figure 5 illustrates the gimbaling of the aeroshell and the resulting shift in center-of-mass. The method of bank angle control for ADEPT is different than the traditional method, where the lift vector is controlled by rotating the entry vehicle using a reaction control system.

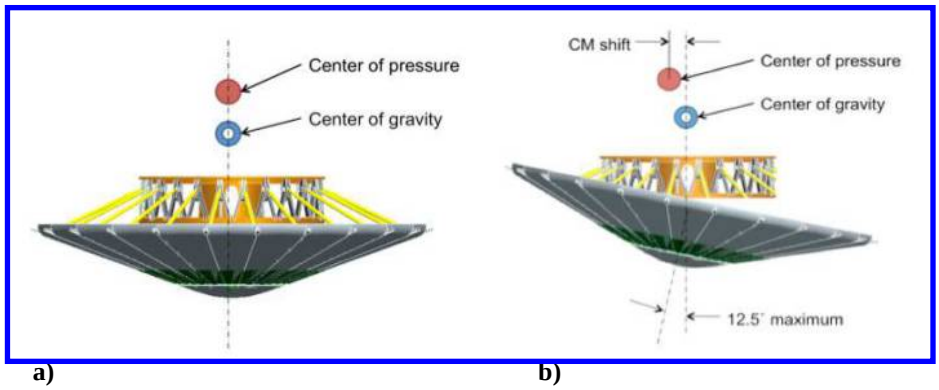

a) **b)**

Figure 5. a) Ungimbaled aeroshell: The center of pressure and center of mass are aligned along the aeroshell axis, trimming the vehicle at 0 deg. angle-of-attack.. b) Gimbaled aeroshell: There is a shift in center of mass and center of pressure, trimming the vehicle at a non-zero angle-of-attack. Bank angle is controlled by gimbaling about the yaw axis.[5]

B. Drag Modulation

This control methodology involves actively controlling the level of deployment of the mechanical decelerator. The decelerator angle is 70 deg. and 45 deg. when it is fully deployed and retracted respectively as shown in Fig. 6. The fully deployed decelerator corresponds to minimum-β, and fully retracted corresponds to maximum-β configurations respectively. When retracted, sag due to lack or pre-tension, local wrinkling, and deflections of the 3D woven cloth due to large pressure loads are neglected. Since the vehicle is in ballistic flight throughout the trajectory, it produces no lift. The drag coefficient depends on the decelerator angle, hence the name drag modulation. Controlling the level of deployment of the decelerator can help contain g-loads within tolerable limits.

As the aerodynamic forces increase, the decelerator retracts to contain the g-loads, and redeploys when the

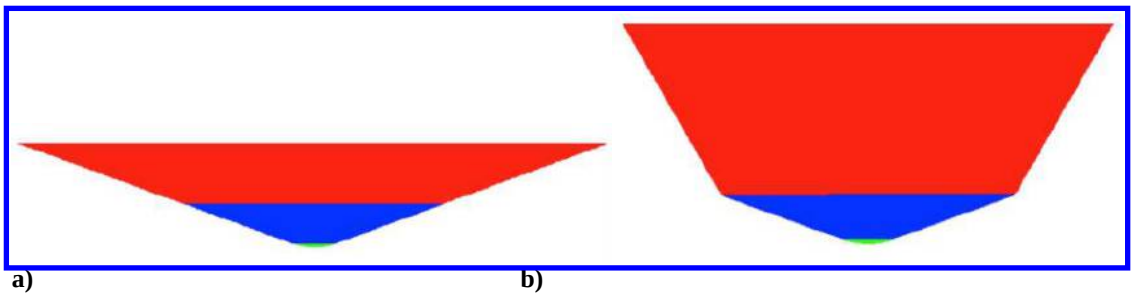

a) **b)**

Figure 6. a) Decelerator (colored red) fully deployed (70 deg.) b) Decelerator fully retracted (45 deg.). The possibility of 3D woven cloth sag due to lack or pre-tension, local wrinkling, and deflections due to large pressure loads are neglected.[6]

aerodynamic forces decreases. One of the potent disadvantages for drag modulation control is that there are no lateral forces generated so it cannot be used for out-of-plane maneuvers unless bank angle control is also used. Drag modulation is achieved by changing the drag skirt deployment angle. For the 23 m ADEPT (architecture #2), and drag modulation control method, the bounds in the control is between 123 kg/m^2 and 365 kg/m^2. For the 44 m ADEPT, the minimum and maximum ballistic coefficients corresponding to decelerator deployment angles of 70 deg. and 45 deg. are 34 kg/m^2 and 104 kg/m^2 respectively.

C. Modified Drag Modulation

Modified drag modulation is similar to drag modulation, except that the aeroshell is permanently gimbaled in a particular direction, resulting in a permanent offset in center-of-mass with respect to the axis of symmetry of the aeroshell. The offset in center-of-mass results in a non-zero trim angle-of-attack, enabling the vehicle to generate lift. The trim angle-of-attack can be varied by controlling the level of deployment of the decelerator. The trim angle-of-attack increases when the decelerator is deployed more, and vice-versa. One important assumption that is made in this control strategy is that the vehicle instantaneously trims to the new angle-of-attack when the decelerator angle is varied, without any transient oscillations. The modified drag modulation control strategy is illustrated in Fig. 7.

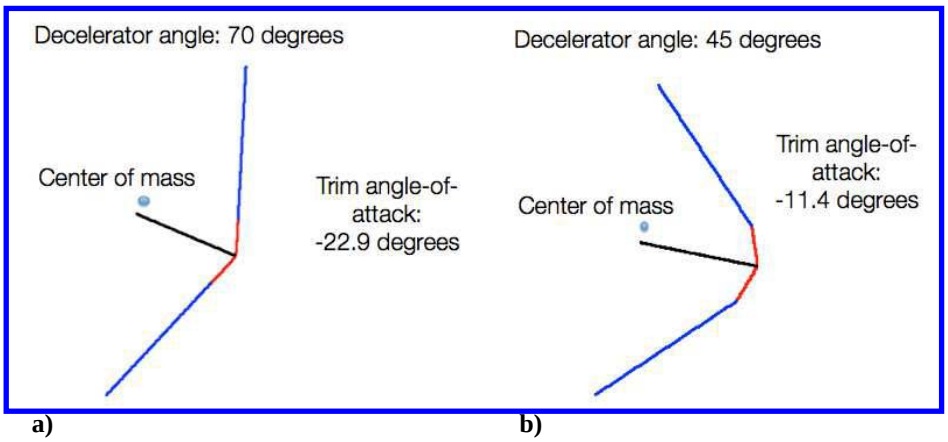

a) **b)**

Figure 7. a) Decelerator fully deployed b) decelerator deployed to 45 degrees. In both the cases, the trim angle of attack changes according to the change in center of mass.

D. Angle-of-Attack, Bank Angle, and Decelerator Deployment Angle Control

This control strategy combines gimbaling of the aeroshell with controlling the level of deployment of the mechanical decelerator. Gimbaling of the aeroshell provides control over bank angle and angle-of-attack, and controlling the deployment of the decelerator provides further control over the coupled lift and drag forces. This control strategy will be the most complex of all. However, it might result in better trajectories and can be advantageous from a guidance perspective because of additional control authority.

VI. Trajectory Optimization Methodology

A. Aerodynamics and Atmosphere Models

Newtonian flow theory is used to compute the aerodynamic coefficients of ADEPT to improve computational speed while performing trajectory optimization.[10] The possibility of 3D woven cloth sag due to lack or pre-tension, local wrinkling, and deflections due to large pressure loads are neglected while computing the aerodynamics coefficients. For Mars missions, an exponential atmosphere model is used with a scale height of 7.1 km and a surface density of 0.02 kg/m^3. For Venus in situ mission, a nominal density profile of Venus-GRAM[11] is used.

B. Trajectory Optimization

Trajectory optimization was performed using Gauss Pseudospectral Optimization Software (GPOPS),[12] which is a general purpose optimal control software. GPOPS converts the continuous time optimal control problem into a nonlinear programming problem, which is then solved using IPOPT. Using each control strategy, the trajectory was

optimized to minimize the stagnation point heat-load. Minimizing the stagnation point heat load results in the minimization of the peak g-load.

1. *Mars Human-Class Missions*

The initial conditions were fixed at a velocity of 5.6 km/s, and an altitude of 120 km. The terminal condition was set at Mach 1.5. It is expected that the supersonic retropropulsion system is capable of producing higher deceleration than the supersonic parachute on Mars Science Laboratory, which justifies the slightly higher final velocity. The vehicle was constrained not to descend below 10 km altitude.

2. *Venus In Situ Missions*

For ADEPT-VITaL, an entry mass of 1602 kg is carried. The entry vehicle carries the scientific payload from entry interface with a velocity of 10.8 km/s to subsonic (Mach 0.8) parachute deployment altitude above 75 km.

In both the cases, the peak g-loads are constrained not to exceed a particular value. The optimization is performed iteratively, and after each iteration, the g-load constraint is tightened to the lowest possible value which yields a feasible solution. The optimizer selects the best entry flight path angle which minimizes the stagnation point heat-load. The trajectory optimization methodology is shown in the schematic in Fig. 8.

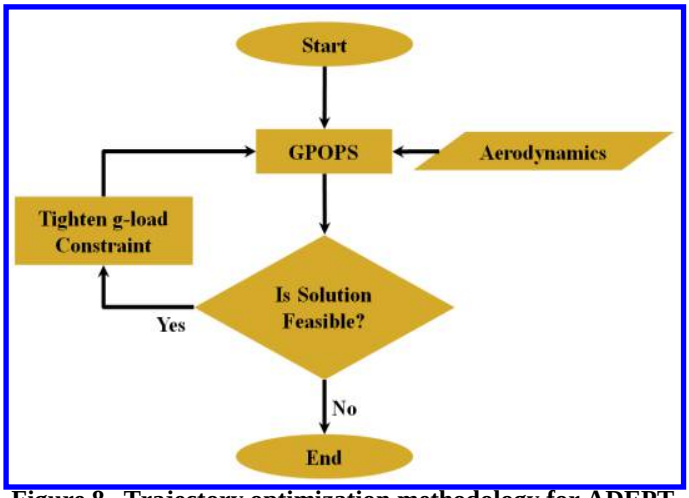

Figure 8. Trajectory optimization methodology for ADEPT using GPOPS.[12] Newtonian flow theory is used to compute the aerodynamic coefficients.[10]

C. Problem Statement

The entry spacecraft is modeled as a point mass over a spherical non-rotating Earth. The entry differential equations of motion are taken from Ref. 13. The objective of the optimal control problem is to minimize the stagnation point heat-load. This objective is mathematically stated as:

$$\text{Min} \quad J = \int_0^{t_f} k\sqrt{\frac{\rho}{R_n}}V^3\,dt \tag{2}$$

Where, k is thermal conductivity in W/m-K; R_n is the spacecraft nose radius; ρ is the atmospheric density; and V is the spacecraft velocity. The value of k for Mars and Venus is 1.9027×10^{-4} W/m-K. The objective is to determine the trajectory and control of the entry vehicle from entry interface to terminal conditions which minimize the objective functional given by Eq. (2) and satisfies the peak g-load constraint η_c such that,

$$\eta_{\max} \le \eta_c \tag{3}$$

and the control should conform to

$$u_L(t) \le u(t) \le u_U(t) \tag{4}$$

where, the control *u(t)* can be any one of the strategies described in Section V.

VII. Results

Using GPOPS, optimal trajectories and control are obtained for human-class Mars missions, and Venus in situ missions. Peak stagnation-point convective heat rate, peak g-load, total stagnation-point heat load, are analyzed while assessing the effectiveness of ADEPT for entry on Mars and Venus. Four control strategies, summarized in Section V are evaluated and compared for human-class Mars missions. For Venus in situ missions, another control method—bank angle modulation—is also considered in the analysis.

A. Human-Class Mars Missions

For human-class Mars missions, two ADEPT architectures to land 40 mt (with an arrival mass of 90 mt) on Mars surface are evaluated. The two architectures are 1) Entry From Mars Orbit Via 23-m ADEPT, and 2) Entry From Mars Orbit Via 44-m ADEPT, where the trajectories in both the cases terminate at supersonic just prior to the initialization of supersonic retropropulsion.

1. Entry From Mars Orbit Via 23-m ADEPT

The comparison of the peak g-load load corresponding to the trajectory that minimizes the stagnation point convective heat load is shown in Fig. 9a. Among the the four control strategies, angle-of-attack (aoa) and bank angle control method yields the trajectory with the minimum peak g-load of little less than 2.5 *g*. The maximum peak deceleration of 4 *g* is found in the case where the three controls are combined: angle-of-attack, bank angle, and decelerator angle (to be referred as 'three-controls method' henceforth).

The cost function is the stagnation point heat load, which is to be minimized. Heat load determines the amount of thermal protection system mass on a entry spacecraft. The three-control method in reality should yield the minimum peak g-load. If the cost function is changed (say to minimize g-load), the three controls-method would perhaps yield the optimal trajectory for minimum peak g-load lower than 4 *g*. Nonetheless, the range of minimum peak g-load, for all the four control strategies is between 2.5 *g* to 4 *g*. The small range in g-load implies that, for the cost function defined in Eq. (2), having a complicated three-controls strategy does not necessarily offer advantages over a simple angle-of-attack and bank angle control strategy. Since, en route to Mars on a 6-months trip to Mars, humans will be deconditioned. As such humans' g-load tolerance capability will reduce. For Apollo missions, the peak g-load during Earth reentry was between 6 *g* to 7 *g*. for Mars entry, the constraint on peak g-load is a fair limitation.

The stagnation-point heat-rate (or heat-flux) for all the control strategies are shown in Fig. 9b. It is clear that the same trajectory using aoa and bank angle control yields both the minimum peak g-load and minimum heat-flux rate of 33 W/cm^2. The peak heat-flux rates for all the control strategies lie between 33 W/cm^2 to around 51 W/cm^2. Even the maximum value of heat flux rate, 51 W/cm^2, is lower than the heat flux rate (< 200 W/cm^2) for Mars Science Laboratory mission.[1] The heat rate represent benign aerothermal environment during entry of ADEPT and much lower than the aerothermal capability of 3D woven carbon cloth which has been tested in arcjet at 136 W/cm^2 at NASA Ames Research Center, and at 246 W/cm^2 at NASA Johnson Space Center.[14] The margin in the peak heat flux can take in to account any increased heating owing to sagging, deflections, and wrinkling of the carbon fabric, which is otherwise neglected for the analysis. For comparison, the peak g-load and peak heat rate of for Mars

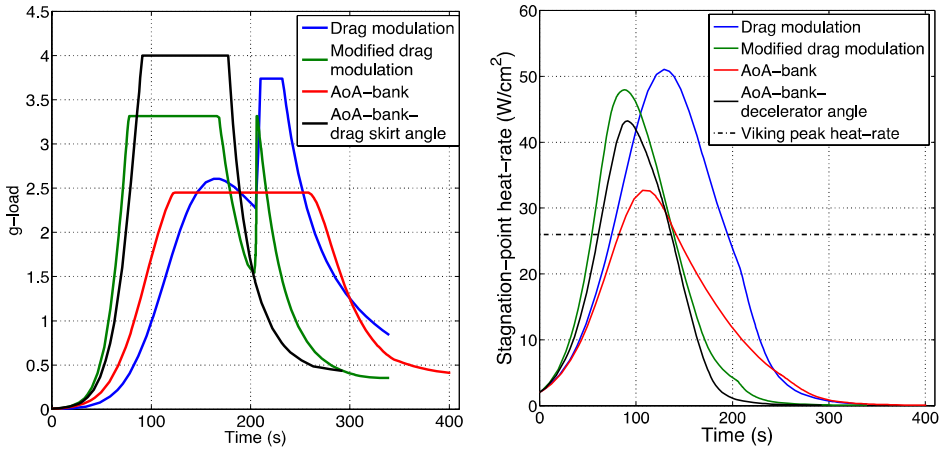

a) **b)**

Figure 9. For 23-m ADEPT entry on Mars, for four different control methods: a) deceleration (g-load) in Earth g's b) stagnation-point heat rate in W/cm^2. The plots are for optimal trajectory solutions where the stagnation point heat load and variable g-load constraint.

Science Laboratory are 15 *g* and 200 W/cm^2 respectively.

The total heat loads at the stagnation point of trajectories corresponding to all the four control methods are shown in Fig. 10a. It is clear that the three-control method produces the trajectory with the minimum stagnation point heat load as the optimizer tries to shorten duration (minimize heat load) of the trajectory still bounded my g-load constraint. The minimum total stagnation-point heat load is 4000 J/cm^2, which is slightly higher than those encountered in the EDL of the Mars Exploration Rovers Spirit and Opportunity.[1] The maximum heat load is for the drag modulation control method is 1.65 times more than the minimum heat load possible. The fact that the aoa-bank angle control method produces the trajectory with minimum peak g-load is clear from the altitude-velocity plot in Fig. 10b: ADEPT using aoa-bank angle control decelerates higher up in the atmosphere flying a shallow flight path angle to meet the constraint of peak g-load, and lowest peak heat flux of 33 W/cm^2.

Considering that the angle-of-attack and bank angle control yields the "best" trajectory, the history of the two control variables are shown in Figs. 11a and 11b. Figure 9b shows nature of bank angle control is a distinctive on-off, bang-bang control.

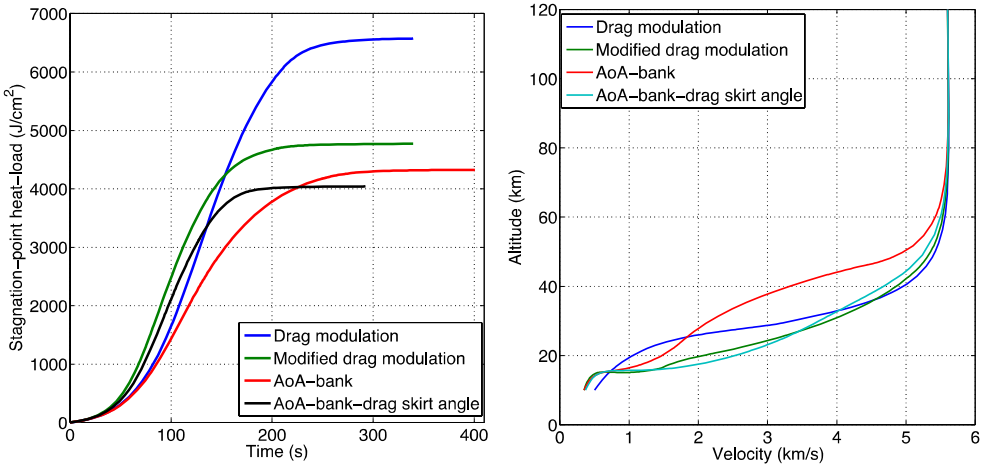

a) **b)**

Figure 10. For 23-m ADEPT entry on Mars, for four different control methods: a) stagnation-point heat load in J/cm^2 b) altitude vs. velocity.

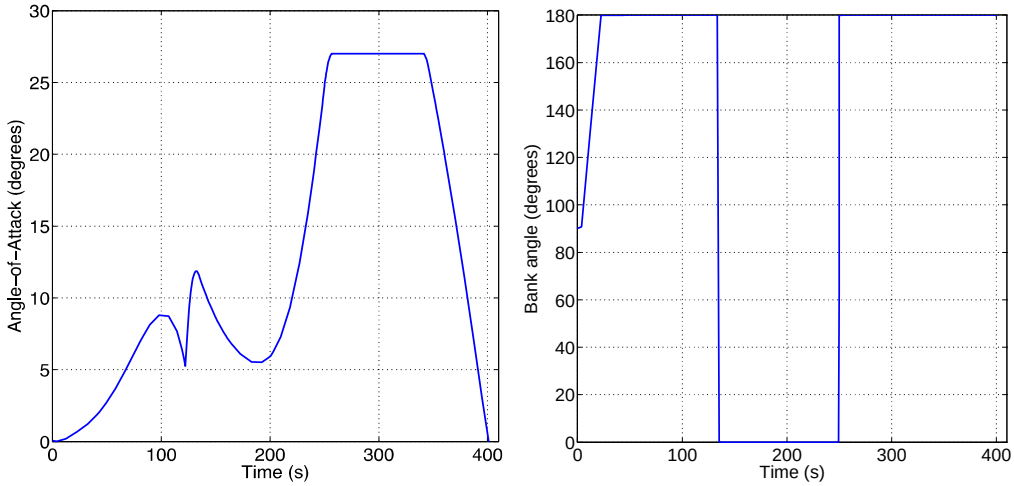

a) **b)**

Figure 11. For 23-m ADEPT entry on Mars for the angle-of-attack and bank angle control method a) profile of angle-of-attack, and b) profile of bank angle showing bang-bang control.

2. Entry From Mars Orbit Via 44 m ADEPT

Compared to a 23-m ADEPT, for the architecture #1, in Fig. (1), a 44 m ADEPT is used for entry on Mars. Logically, a 44-m ADEPT will lead to further decrease in ballistic coefficient. The variation of the ballistic coefficient as a function of ADEPT diameter is shown in Fig. 12. The arrival mass is assumed to be 90 mt for which the ballistic coefficients are computed using Eq. (1).

The line in the plot corresponding to deceleration angle of 70 deg. is when ADEPT is fully deployed. In the drag modulation control, as the decelerator deployment angle is controlled between 70 deg. and 45 deg.. The minimum decelerator deployment angle assumed is 45 deg., beyond which the decelerator may touch the payload. The range of large ballistic coefficients is when the decelerator is retracted to 45 deg.

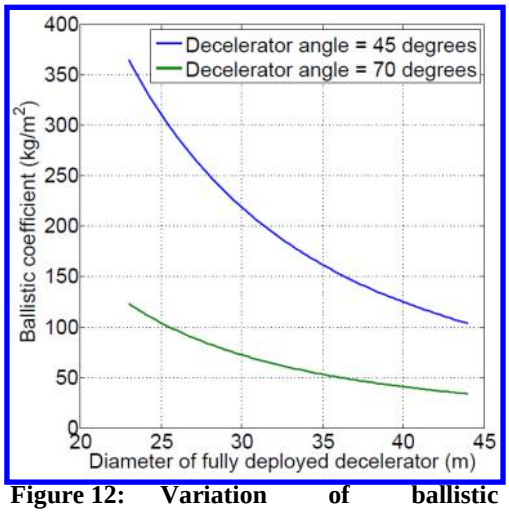

Figure 12: Variation of ballistic coefficient as a function of ADEPT diameter for a 90 mt arrival mass. The diameter corresponds to when ADEPT is fully deployed. Each plot corresponds to a value of the decelerator deployment angle.

Figure 13 shows the plot of g-load as a function of time for the four control strategies for the case of 44-m ADEPT. It is evident that lowering the ballistic coefficient by increasing the reference area reduces the peak g-load by more than half. In fact, it is possible to land on Mars with the peak deceleration of around 1 *g* for both the modified drag modulation and three control method. The two peaks of the g-load curve for the drag modulation control method hints at the 'skip' nature of the trajectory. Therefore, there is a limit to the minimum peak g-load achievable using any control method before the spacecraft skips out to meet the g-load constraint. On the other hand, for human missions to Mars, it is beneficial to maintain the g-load profile within the human tolerance. The 44 m ADEPT also results in the reduction of peak heat flux as compared to the 23 m ADEPT. The minimum peak heat flux is found to be 13 W/cm^2 for the three control method, less than half of the minimum peak g-load value for the 23 m case. The peak heat flux values for the four control methods are between 13 W/cm^2 and 23 W/cm^2, and is well below the 250 W/cm^2 thermal capability of 3D woven cloth TPS. The stagnation point heat load of 2750 J/cm^2 is lowest for drag modulation, and angle-of-attack and bank

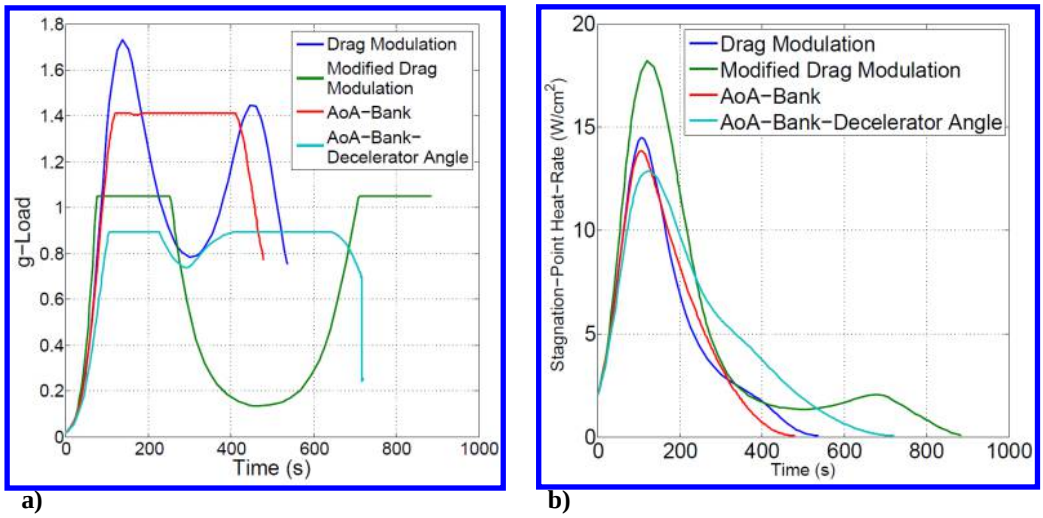

a) **b)**

Figure 13. For 44-m ADEPT entry on Mars, for four different control methods: a) g-load in Earth g's, plot with two peaks denotes skip nature of trajectory b) stagnation-point heat rate in W/cm^2. The plots are for optimal trajectory solutions where the stagnation point heat load and variable g-load constraint.

angle control methods. The three control method, which yields the minimum peak g-load and minimum peak heat flux, results in to a total heat load of 3550 J/cm^2. The maximum heat flux of 4150 J/cm^2 is for the case of modified drag modulation control method.

B. Venus In Situ Missions

In addition to the four control methods outlined in Section V, simple bank angle control method is assessed instead of modified drag control for Venus in situ mission using ADEPT. All the previous US Venus missions, the peak deceleration is more than 220 *g* and peak heat rate greater than 3 kW/cm^2. Dutta et al. showed that use of lower ballistic coefficients (< 30 kg/m^2) could lead to order of magnitude decrease in the peak g-load. ADEPT-VITaL demonstrated that the peak g-load reduces to 30 *g* for ballistic entry.[4]

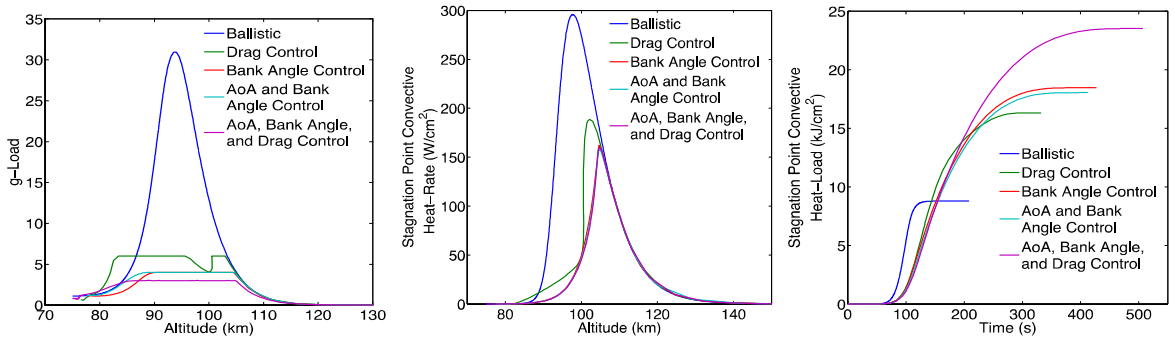

a) **b)** **c)**

Figure 14. 6 m / 70º ADEPT for Venus in situ missions: a) g-load b) stagnation-point convective heat rate c) total convective heat load. Bank angle control is assessed in lieu of modified drag modulation.

Figure 14a shows the comparison of peak g-load for ballistic entry and four different control methods of ADEPT-VITaL. It becomes very clear that the three control method yields the solution with minimum peak g-load of 3 *g*. The reduction in peak g-load represents a further order of magnitude reduction compared to the ADEPT ballistic entry case. It is interesting to see that for Venus entry, the peak g-load for all the four control methods lie between 3 *g* to 6 *g*.

In Fig. 14b, the the peak heat flux corresponding to all the control methods are shown. Compared to the heat rate of 300 W/cm^2 for ballistic entry, use of guided entry results in to heat flux rates between 160 W/cm^2 to 180 W/cm^2, again within the thermal capability of 3D woven carbon cloth. All the control methods result in to very similar heat rates of around 160 W/cm^2, while the rate is somewhat higher for the case of drag modulation. Therefore, from g-load and peak heat rate point of view, it can be seen that a particular control method does not offer significant advantage over another.

On the other hand, since the atmosphere of Venus is very dense, the total stagnation-point convective heat load is significantly higher. Since, the entry flight angle for the ballistic entry case is steeper, the heat load is less compared to the cases when control is used as the vehicle flies a shallower flight path angle to meet the g-load constraint. The range of heat load is from 16 kJ/cm^2 to 23 kJ/cm^2 as shown in Fig. 14c.

A note on the history of control commands for different methods is as follows. Figure 15a shows the drag skirt deployment angle which characterizes the drag modulation of ADEPT for Venus mission. ADEPT is partically retracted to 55 deg. at entry interface and stay mostly fully deployed at 70 degrees. The delecerator is retracted when the g-load continues to increase as the spacecraft descends and aerodynamic forces increases. For the angle of attack and bank angle control method, the control histories are shown in Fig. 15b and Fig. 15c.

The bank angle profile can be easily identified as the traditional bang-bang control. The angle of attack profile has a number of high-frequency variations owing to density variations in the VenusGRAM used in the optimization. From system point of view, a low-pass filter can be used to smooth the high-frequency disturbances.

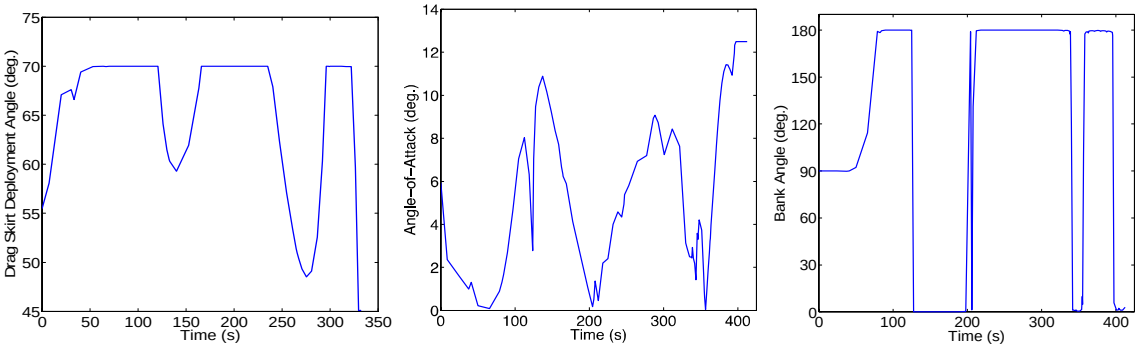

(a) **(b)** **(c)**

Figure 15. 6 m / 70º ADEPT for Venus in situ missions for four different control strategies: a) drag skirt deployment angle (drag modulation) history b) angle-of-attack, and c) bank angle modulation. The high frequency variations in angle-of-attack is due use of Venus-GRAM.

VIII. Discussions

For a fully deployed 23-m ADEPT the ballistic coefficient is 123 kg/m^2, and 34 kg/m^2 for a 44-m ADEPT. For the 23-m ADEPT, the simple angle of attack and bank angle control method is capable of delivering 40 mt on Mars with a benign entry environment, where the peak g-load is less than 2.5 *g* and peak heat flux rate is 33 W/cm^2. Low peak g-load is preferred for human mission to Mars, as after more than 6 months trip to Mars, humans after being deconditioned, the g-load tolerance capability will be lower. Using a 44-m ADEPT, peak g-load can be further decreased to a comfortable 1 *g* entry on Mars.

The minimum peak heat flux rate for 44-m ADEPT is 13 W/cm^2, as opposed to 33 W/cm^2 for the 23-m ADEPT. The peak flux heat rate is far less than the thermal capability of 3D woven carbon cloth. The stagnation point heat load determines the mass of the thermal protection system. The minimum heat loads for the 23 m and 44 m are 2750 J/cm^2 and 4000 J/cm^2, comparable to or less than heat load of Mars Phoenix mission.[1] Depending on the performance of the control methods, as well as the system mass and complexity, the right control method for lifting and guided entry can be selected.

Ballistic entry on Venus using low ballistic coefficient (< 30 kg/m^2) ADEPT results in order of magnitude reduction in the peak g-load (from > 200 *g* to 30 *g*) and stagnation point heat flux rate (from >3000 W/cm^2 to 300 W/cm^2).[4] Results in this study indicate that use of lifting and guided entry result in further order of magnitude reduction in the peak g-load to less than 6 *g* and as low as 3 *g*. At the same time, guided entry results in around 50% reduction in the peak heat rate to 160 W/cm^2, compared to a ballistic entry. Use of three control method results in the minimum peak g-load and peak heat flux rate.

The advantages of low peak g-load are manifold:

a. Reduction of entry loads leads to decrease in structural mass of the spacecraft, and payload support mechanisms.
b. Due to reduction of deceleration loads, similar to seen for Mars entry; therefore sensitive science instruments could be included, not otherwise possible when rigid aeroshell technology is used.
c. Overall mass savings due to reduction in the deceleration loads can be used (1) for an improved thermal management system for surface operations of the lander, (2) increase mass for instrument suite, (3) and reduced launch vehicle requirements.
d. With low peak g-load, there is no requirement to develop instrument systems to withstand extremely high loads; thereby saving millions of dollars in development and research cost.

The peak heat flux of ADEPT-VITaL of 160 W/cm^2 is less than the current capability of 3D woven carbon cloth at 250 W/cm^2. That is, there is a considerable margin in heat rate when guided entry is considered, as opposed to ballistic entry using ADEPT. For Venus missions, all the control methods, offer similar perfomances in terms of peak g-load and peak heat rate. Therefore, total heat load, as well as system mass and complexity may be used to select the right control method for lifting and guided entry. At the same time, for drag modulation, there are no lateral forces generated so drag control cannot be used for out of plane maneuvers unless bank angle control is also used.

IX. Conclusions

Results indicate that ADEPT is an enabling alternative to the traditional aeroshell technology for entry, descent, and landing of spacecraft of Mars and Venus. ADEPT aids in reduction of the ballistic coefficient and shallower entry flight angles become practicable. Consequently, as deceleration occurs at much higher altitudes, an entry vehicle is subjected to lower peak g-load, lower heating, aerodynamic pressure, and total heat load.

ADEPT also presents attractive options of lifting and guided entry using various control methods. One of the primary methods is the angle of attack and bank angle control via the gimbaling of the decelerator surface. Additionally, a new control method of drag modulation is considered which is achieved by controlling in the level of deployment of the decelerator surface. The extrema in the level of deployments correspond to minimum (when fully deployed) and maximum (when fully retracted) ballistic coefficients respectively. ADEPT presents a very benign entry environment in terms of peak deceleration and peak heat rates for both human Mars and Venus in situ missions. For lifting and guided entry for Venus in situ missions, ADEPT could lead to a two-order-of-magnitude decrease in peak deceleration and to a 50% decrease in peak heat-flux compared to conventional rigid aeroshell technology.

Finally, many interesting targets on Venus—Cleopatra, Maat Mons, interiors of craters, young flows etc.—may require precision landing. ADEPT has the capability of incorporating guidance using one of the control methods outlined in Section V for precision landing.

References

[1]Braun R. D., and Manning R. M., "Mars Exploration Entry, Descent, and Landing Challenges," *Journal of Spacecraft and Rockets*, Vol. 44, No. 2, March–April 2007.

[2]Dwyer-Cianciolo, A. M., Davis, J. L., Komar, D. R., Munk, M. M., Samareh, J. A., Williams-Byrd, J. A., Zang, T. A., Powell, R. W., Shidner, J. D., Stanley, D. O., Wilhite, A. W., Kinney, D. J., McGuire, M. K., Arnold, J. O., Howard, A. R., Sostaric, R. R., Studak, J. W., Zumwalt, C. H., Llama, E. G., Casoliva, J., Ivanov, M. C., Clark, I., and Sengupta, A., "Entry, Descent and Landing Systems Analysis Study: Phase 1 Report," NASA/TM-2010-216720, July 2010, Washington D.C.

[3]Dwyer-Cianciolo, A. M., Davis, J. L., Engelund, W. C., Komar, D. R., Queen, E. M., Samareh, J. A., Way, D. W., Zang, T. A., Murch, J. G., Krizan, S. A., Olds, A. D., Powell, R. W., Shidner, J. D., Kinney, D. J., McGuire, M. K., Arnold, J. O., Covington, M. A., Sostaric, R. R., Zumwalt, C. H., and Llama, E. G., "Entry, Descent and Landing Systems Analysis Study: Phase 2 Report on Exploration Feed-Forward System," NASA/TM-2011-217055, February 2011, Washington D.C.

[4]Dutta, S., Smith, B., Prabhu, D., and Venkatapathy, E., "Mission Sizing and Trade Studies for Low Ballistic Coefficient Entry Systems to Venus," IEEE Aerospace Conference, Big Sky, MT, April 2012.

[5]Venkatapathy, E., Arnold, J. O., Fernandez, I., Hamm Jr., K. R., Kinney, D., Laub, B., Makino, A., McGuire M. K., Peterson, K., Prabhu, D., Empey, D., Dupzyk, I., Huynh, L., Hajela, P., Gage, P., Howard, A., and Andrews, D., "Adapative Deployable Entry, and Placement Technology (ADEPT): A Feasibility Study for Human Mission to Mars," 21st AIAA Aerodynamic Decelerator Systems Technology Conference Seminar, 23–26 May, 2011, Dublin, Ireland.

[6]Smith, B., Venkatapathy, E., Wercinski, P., Yount, B., Prabhu, D., Gage, P., Glaze, L., and Baker, C., "Venus In Situ Mission Design using a Mechanically Deployed Aerodynamic Decelerator," Aerospace Conference, 2013 IEEE , Vol., No., pp.1,18, 2-9 March 2013, doi: 10.1109/AERO.2013.6497176.

[7]Squyres, S. et al., "Visions and Voyages for Planetary Science in the Decade 2013-2022 (Decadal Survey)," The National Academies Press, Washington, D.C., 2011. VITaL report.

[8]Gilmore, M.S. et al., "Venus Intrepid Tessera Lander: Mission Concept Study Report to the NRC Decadal Survey Inner Planets Panel," NASA GSFC – NASA ARC, April 2010.

[9]Arnold, J.O., Laub, B., Chen, Y-K., Prabhu, D.K., Bittner, M.E., Venkatapathy, E., "Arcjet Testing of Woven Carbon Cloth for Use on Adaptive Deployable Entry and Placement Technology," IEEE Aerospace Conference, Big Sky, MT, March 2013.

[10]Regan, F. J., and Anandakrishnan, S. M., *Dynamics of Atmospheric Re-Entry*, AIAA Education Series, AIAA, Washington D.C., 1993, Chap. 11.

[11]Venus Global Reference Atmospheric Model (Venus- GRAM 2005 Rel. Oct 2009), NASA Marshall Space Flight Center, Environments Group, EV13, Huntsville, AL.

[12]Rao, A. V., Benson, D. A., Darby, C. L., Francolin, C., Patterson, M. A., Sanders, I., and Huntington, G. T., "Algorithm 902: GPOPS, A Matlab Software for Solving Multiple-Phase Optimal Control Problems Using the Gauss Pseudospectral Method," *ACM Transactions on Mathematical Software*, Vol. 37, No. 2, April–June 2010, Article 22, p. 39.

[13]Vinh, N.-X., Busemann, A., and Culp, R. D., *Hypersonic and Planetary Entry Flight Mechanics*, Univ. of Michigan Press, Ann Arbor, MI, 1980, pp. 4–28.

[14]Arnold, J.O., Laub, B., Chen, Y-K., Prabhu, D.K., Bittner, M.E., Venkatapathy, E., "Arcjet Testing of Woven Carbon Cloth for Use on Adaptive Deployable Entry and Placement Technology," IEEE Aerospace Conference, Big Sky, MT, March 2013.